CrossMark

Joanne C. McNelis,[1] Yun Sok Lee,[1] Rafael Mayoral,[1] Rik van der Kant,[2] Andrew M.F. Johnson,[1] Joshua Wollam,[1] and Jerrold M. Olefsky[1]

GPR43 Potentiates β-Cell Function in Obesity

ISLET STUDIES

The intestinal microbiome can regulate host energy home- ostasis and the development of metabolic disease. Here we identify GPR43, a receptor for bacterially produced short-chain fatty acids (SCFAs), as a modulator of microbiota-host interaction. β-Cell expression of GPR43 and serum levels of acetate, an endogenous SCFA, are increased with a high-fat diet (HFD). HFD-fed GPR43 knockout (KO) mice develop glucose intolerance due to a defect in insulin secretion. In vitro treatment of isolated murine islets, human islets, and Min6 cells with (S)-2- (4-chlorophenyl)-3,3-dimethyl-*N*-(5-phenylthiazol-2-yl) butanamide (PA), a specific agonist of GPR43, in- creased intracellular inositol triphosphate and Ca^{2+} levels, and potentiated insulin secretion in a GPR43-, Gαq-, and phospholipase C–dependent manner. In ad- dition, KO mice fed an HFD displayed reduced β-cell mass and expression of differentiation genes, and the treatment of Min6 cells with PA increased β-cell prolifera- tion and gene expression. Together these findings identify GPR43 as a potential target for therapeutic intervention.

The prevalence of type 2 diabetes (T2D) has risen dramat- ically in recent decades, becoming a global epidemic that affects ~6% of the adult population of the world. The progression to overt T2D requires the development of both insulin resistance and impaired β-cell function (1). Obesity is the most common cause of insulin resistance, but overt diabetes does not develop in the majority of obese individ- uals, as they can preserve normoglycemia through an adap- tive increase in β-cell mass and enhanced insulin secretion, resulting in compensatory hyperinsulinemia (2). However, in susceptible individuals compensatory hyperinsulinemia cannot be maintained, and hyperglycemia and T2D develop (3). Therefore, therapeutic strategies that maintain β-cell mass and promote β-cell function are of intense interest.

β-cell mass is dependent on the dynamic balance of β-cell proliferation, β-cell hypertrophy, β-cell neogenesis, β-cell apoptosis, and the transdifferentiation of β-cells to and from other cell types (4–6). Longitudinal studies of murine T2D models have shown that β-cell mass initially expands as insulin resistance develops, owing to prolifera- tion, but then subsequently declines, owing to increased apoptosis and dedifferentiation of β-cells to endocrine progenitor cell types (6,7). Similar findings have been reported in humans—β-cell mass correlates with BMI in individuals with normal glucose tolerance, but is re- duced in individuals with diabetes (5). The β-cell com- pensatory response also involves functional adaptations that result in insulin hypersecretion. As T2D develops, β-cell insulin secretion capacity is reduced, contributing to the relative insulin deficiency (1,3).

Recently, the intestinal microbiome has emerged as an important regulator of host metabolic function. Micro- biota dysbiosis can influence the development of obesity, insulin resistance, and diabetes (8–13) through several mechanisms, including the production of bioactive metab- olites. Short-chain fatty acids (SCFAs) (acetate, butyrate, and propionate) are among the most abundant microbiota- derived metabolites, and are produced through the fermen- tation of dietary fiber and resistant starch that cannot be metabolized by the host. In obesity, the microbiome is enriched for enzymes involved in polysaccharide metabo- lism, and obese mice and humans exhibit elevated fecal SCFA levels (10,14). Once produced, SCFAs enter the cir- culation and can be used for de novo lipid or glucose syn- thesis (15,16), such that the microbiota, through the production of SCFAs, can provide up to 5–10% of human daily energy intake (17).

In addition to their role as metabolic substrates, SCFAs can act as signaling molecules through G-protein–coupled

[1]Division of Endocrinology and Metabolism, Department of Medicine, University of California, San Diego, La Jolla, CA
[2]Department of Cellular and Molecular Medicine, University of California, San Diego, La Jolla, CA

Corresponding author: Jerrold M. Olefsky, jolefsky@ucsd.edu.

receptors, including GPR43 (FFAR2) and GPR41 (FFAR3). GPR43 is dual coupled to both Gαq and Gαi, resulting in the activation of phospholipase C (PLC) β and increased intracellular calcium levels, or the inhibition of cAMP production by adenylate cyclase, respectively. GPR43 is highly expressed by intestinal epithelial cells (18), immune cells (19,20), adipocytes (21,22), and pancreatic islets (23–26), and is upregulated in islets during pregnancy (27). A number of studies have implicated GPR43 in the regulation of intestinal homeostasis and inflammation, but the role of GPR43 beyond the intestine is less clear. GPR43 activation has been reported to promote leptin secretion (22) and adipogenesis (28), and can have both stimulatory and inhibitory effects (21) on adipose tissue insulin signaling. Furthermore, the activation of GPR43 can promote the secretion of glucagon-like peptide 1 (GLP-1) from L cells (29). However, a direct effect of GPR43 activation by SCFAs in pancreatic β-cells has not been explored. In this study, we demonstrate a regulatory pathway for the SCFA/GPR43 axis in the modulation of β-cell function. We show that GPR43 knockout (KO) mice exhibit both reduced β-cell function and mass in response to a high-fat diet (HFD). Furthermore, we demonstrate that a small-molecule agonist for GPR43 increases insulin secretion, suggesting a therapeutic potential for GPR43 agonists in the treatment of T2D.

RESEARCH DESIGN AND METHODS

Mice
GPR43 KO mice were generated by targeted deletion by Lexicon Genetics, as previously described (30), and were provided by Amgen Inc. Heterozygous mice were crossed to generate wild-type (WT) and KO littermates. After weaning, genotypes were housed separately to permit analysis of fecal microbiota. Only male mice were used for experiments. Mice were fed standard chow (13.5% fat; LabDiet) or an HFD (60% kcal from fat; catalog #D12492; Research Diets) from 8 weeks of age. Procedures involving mice were performed in accordance with the *Guide for Care and Use of Laboratory Animals* of the National Institutes of Health, and were approved by the Animal Subjects Committee of the University of California, San Diego.

GPR43 Agonists
The specific small-molecule GPR43 phenylacetamide agonist (S)-2-(4-chlorophenyl)-3,3-dimethyl-*N*-(5-phenylthiazol-2-yl)butanamide (PA), described as compound 58 in the study by Wang et al. (31), was obtained from Merck Millipore (catalog #371725) and used at 1 μmol/L for all experiments. Sodium acetate was used at 1 mmol/L for all experiments.

Metabolic Tests
For metabolic analysis of WT and KO mice, glucose tolerance tests (GTTs), arginine tolerance tests, and insulin tolerance tests were performed on 6 h–fasted mice, as previously described (32). For GTTs, 1 g/kg dextrose

was administered by intraperitoneal injection or oral gavage. For insulin tolerance tests, insulin was administered (normal chow [NC] 0.35 units/kg, HFD 0.6 units/kg) by intraperitoneal injection. Arginine (1 g/kg) was administered by intraperitoneal injection.

In Vivo Labeling With BrdU
BrdU was administered at 1 mg/mL for 4 weeks in the drinking water during HFD feeding (weeks 8–12 of the HFD). To ensure that the BrdU remained bioactive, water bottles were covered in aluminum foil and were changed weekly.

Histological Analysis
After antigen retrieval, deparaffinized pancreatic tissue sections were blocked with normal donkey serum and immunostained with anti-insulin (N1542; Dako North America, Carpinteria, CA), anti-glucagon (PA1–85465; Pierce Chemical Company, Rockford, IL), anti-GPR43 (PAB16402; Abnova), or anti-BrdU (ab6326; Abcam), followed by incubation with secondary antibodies conjugated with Alexa Fluor 488 or Alexa Fluor 594 and counterstained with DAPI. For β-cell mass analysis, images were captured using a Hamamatsu NanoZoomer HT-2.0 slide scanner and were analyzed using Image-Pro Plus software. A minimum of five slides per animal, 100 μm apart, were used to quantify the relative pancreatic β-cell area, by dividing the total pancreatic area by the insulin-positive (Ins$^+$) area. The percentage of proliferating β-cells was calculated by dividing the number of BrdU-positive (BrdU$^+$) and Ins$^+$ cells by the number of Ins$^+$ cells.

Thymidine Incorporation Assays
After isolation, 20 islets per well were cultured in the presence of GPR43 agonists (1 mmol/L acetate or 1 μmol/L PA) and 1 μCi [methyl-^{3}H]-thymidine/mL media. After 48 h of incubation, islets were precipitated in trichloroacetic acid and then lysed in NaOH. Thymidine incorporation was determined by scintillation counting and normalized to total protein content.

Measurement of Insulin Secretory Response From Isolated Islets
Primary murine islets were isolated as previously described (32). For analysis of insulin secretion, 10 islets were hand picked and incubated in Krebs-Ringer buffer with 2.8 or 16.7 mmol/L glucose and 100 nmol/L GLP-1 or GPR43 agonists. Human islets were incubated for 1 h in Hanks' balanced salt solution containing 2.8 or 16.7 mmol/L glucose, with or without GPR43 agonists. Insulin concentrations in the supernatant were determined by ELISA.

Plasma Protein Measurements
Plasma insulin, C-peptide, and GLP-1 levels were measured by ELISA. Plasma glucose-dependent insulinotropic polypeptide (GIP) and peptide YY (PYY) levels were measured by Luminex (Millipore).

Serum Acetate Measurements
Serum acetate concentrations were quantified using the Acetate Colorimetric Assay Kit (BioVision).

Generation of GPR43 Hematopoietic-Deficient Mice

Bone marrow transplants were performed as previously described (33). Briefly, bone marrow obtained from WT and GPR43 KO mice (~4 × 10⁶ cells) was injected through the tail vein into 8-week-old WT mice that had been irradiated (1,000 rad). After 8 weeks, peripheral white blood cells were isolated, and reconstitution of donor marrow was verified by quantitative PCR for GPR43. Mice were then placed on a 60% HFD for 18 weeks.

Min6 Cell Culture

Min6 cells were maintained as previously described (32). Cells were used between passages 16 and 30. For small interfering RNA (siRNA) depletion experiments, cells were transfected with 30 nmol/L siRNA (Dharmacon ON-TARGETplus SiRNA; Thermo Scientific) using PepMute siRNA Transfection Reagent (SignaGen Laboratories). Assays were performed 48 h after transfection.

Measurement of Min6 Proliferation

Min6 cell proliferation was measured using the Click-iT EdU Microplate Assay Kit (Life Technologies).

Measurement of Min6 Apoptosis

Min6 cell apoptosis was measured using the ApoLive-Glo Multiplex Assay (Promega).

Intracellular Inositol Monophosphate Generation

The activation of PLC signaling and inositol triphosphate (IP_3) generation in Min6 cells and isolated islets was measured using the IP-One ELISA (CisBio), which quantifies the accumulation of inositol monophosphate (IP_1), a downstream metabolite of IP_3. Min6 cells, 15 mouse islets or 125 islet equivalent human islets, were incubated in stimulation buffer containing lithium chloride, supplemented with 16.7 mmol/L glucose, for 1 h at 37°C, in 5% CO_2.

Intracellular cAMP Analysis

Intracellular cAMP levels in Min6 cells and isolated islets were measured using Bridge-It cAMP Designer Fluorescence Assay Kit (Medomics). Min6 cells, 15 mouse islets or 62.5 islet equivalent human islets, were incubated in Krebs-Ringer buffer containing 3-Isobutyl-1-methylxanthine and 16.7 mmol/L glucose. cAMP production was stimulated by treatment with 100 μmol/L forskolin.

Gene Expression Analysis

RNA was isolated with TRIzol reagent, and cDNA was synthesized using the High Capacity Reverse Transcription Kit (Applied Biosystems). Quantitative real-time PCR was performed using iTaq Universal SYBR Green Supermix (Bio-Rad) and the StepOnePlus Real-Time PCR system. Relative gene expression was calculated by the ΔΔCt method using GAPDH as an internal control.

Statistics

The results are shown as the mean ± SEM. All statistical analysis was performed using a Student t test in Microsoft Excel or ANOVA with multiple comparisons in GraphPad Prism. A P value of <0.05 was considered significant.

RESULTS

In line with previous studies, quantitative PCR confirmed that GPR43 is abundantly expressed in the murine intestine, adipose tissue, pancreas (Fig. 1A), and isolated islets (Fig. 1B). HFD feeding induced GPR43 expression 3.2-fold in islets, compared with islets from mice fed an NC diet, with a comparable increase in GPR43 expression in adipose tissue (Fig. 1B). Significant GPR43 expression was also detected in the murine Min6 β-cell line and human islets (Fig. 1C). Histological analysis of murine islets confirmed that GPR43 colocalizes with insulin in β-cells (Fig. 1D). HFD feeding increased levels of serum acetate, the most abundant circulating GPR43 ligand, in WT mice (Fig. 1E). As acetate is a product of dietary fiber fermentation, we examined serum acetate concentrations under fasting conditions. As expected, serum acetate levels were reduced after fasting for 24 h (Fig. 1E). No difference in serum acetate concentrations was observed between GPR43 KO and WT mice, fed either an NC diet or an HFD.

It is well documented that obesity is associated with microbiota dysbiosis, notably a decrease in the proportion of Bacteroidetes, and an increase in the proportion of Firmicutes, Gammaproteobacteria, and Actinobacteria, the four most abundant phyla. Consistent with this, using primers specific for the 16S rRNA gene region of each phylum, we observed an increase in Firmicutes and a decrease in Bacteroidetes in the feces of HFD-fed mice (Fig. 1F). In HFD-fed mice, the proportion of Firmicutes (Fig. 1F) and Gammaproteobacteria (Fig. 1H) was higher in WT mice, while the proportion of Actinobacteria was elevated in KO mice (Fig. 1G). There was no difference in Bacteroidetes concentration between WT and KO animals (Fig. 1F). Several bacterial species express the enzymes involved in SCFA production. To assess whether the HFD-induced changes in microbiota are associated with altered enzyme levels, we measured the expression of butyryl CoA transferase (BCoAT) and formyltetrahydrofolate synthase (FTHFS), which catalyze the final steps in butyrate and acetate synthesis, respectively (34). Consistent with the observed increase in serum acetate levels after HFD feeding, levels of FTHFS were increased in KO and WT HFD mice, while levels of BCoAT were significantly increased in WT HFD animals (Fig. 1H).

The adipose tissue and pancreas express high levels of GPR43, which is further upregulated by HFD feeding, thus representing a candidate mechanism by which the microbiome can influence host metabolic functions. Therefore, we evaluated the effect of GPR43 on glucose tolerance in lean and obese KO mice. No difference in body weight was observed between WT and KO mice fed an NC diet (Fig. 2A). After HFD feeding, KO mice trended toward reduced body weight (Fig. 2B), with no difference in food intake (Fig. 2C) or tissue mass of the liver, adipose, or pancreas (Fig. 2D).

KO mice fed a short-term (8-week) NC diet or HFD exhibited normal glucose tolerance (Fig. 2E and F) and
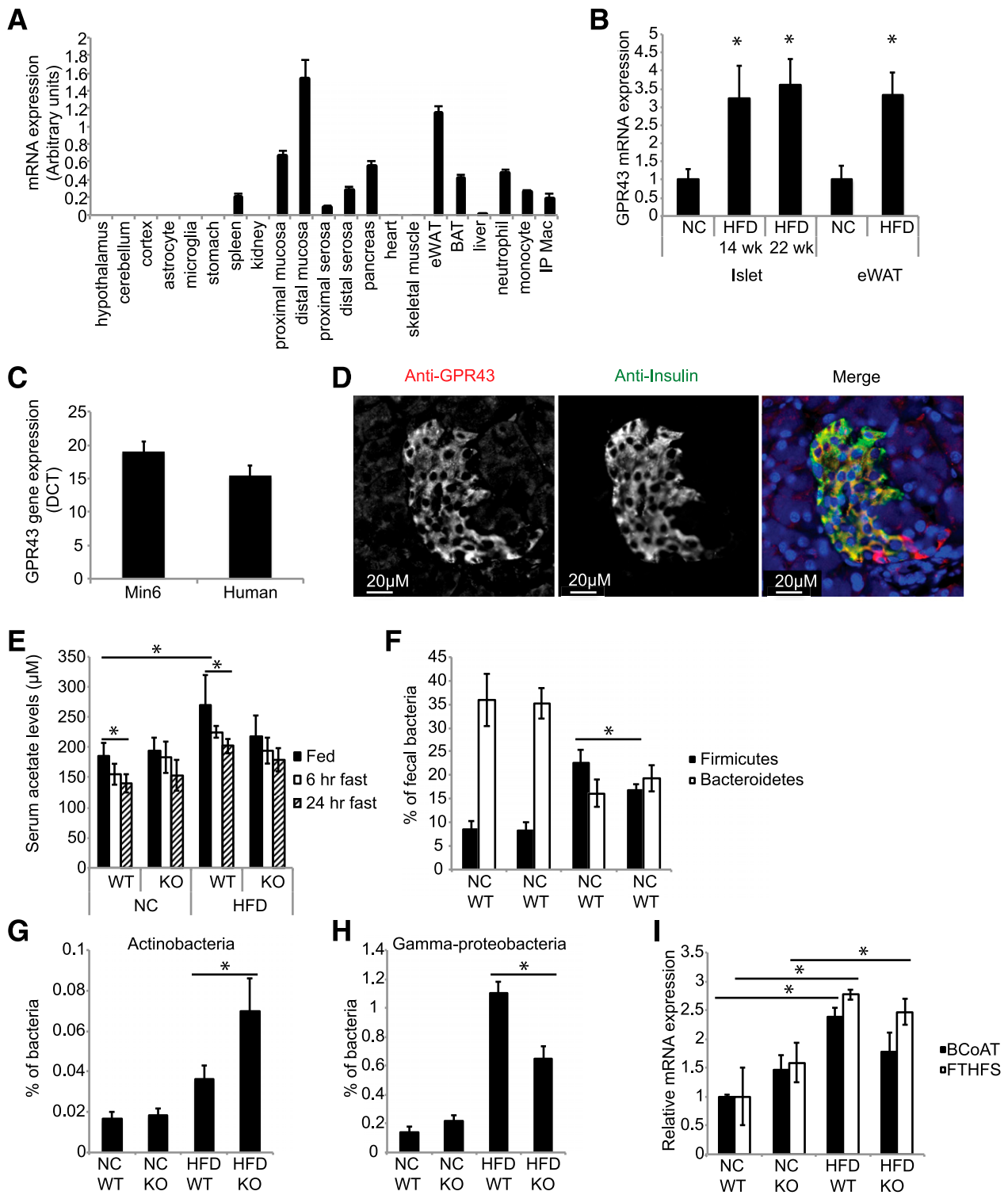
Figure 1—GPR43 is expressed in pancreatic β-cells and is increased by HFD. *A*: GPR43 mRNA expression in murine tissues. BAT, brown adipose tissue; eWAT, epididymal white adipose tissue; IP Mac, intraperitoneal macrophage. Data are reported as the mean ± SEM, $n = 4$. *B*: GPR43 expression in murine islets and eWAT isolated from NC or HFD mice. Data are reported as the mean ± SEM, $n = 4$. *$P < 0.05$, NC vs. HFD. *C*: GPR43 expression in murine and human islets. Data are reported as the mean ± SEM, $n = 4$. *D*: Immunofluorescence analysis of GPR43 expression in murine islets. Anti-GPR43 is shown in red, and anti-insulin is shown in green. *E*: Serum acetate levels in WT and KO mice fed an NC diet and a 14-week HFD, and fasted mice. Data are reported as the mean ± SEM, $n = 6$ per group. *$P < 0.05$. *F–H*: Real-time PCR quantification of fecal bacterial phyla abundance, as a percentage of total bacteria, in WT and KO mice fed an NC diet and a 14-week HFD. *F*: Abundance of Firmicutes and Bacteroidetes. *G*: Abundance of Actinobacteria. *H*: Abundance of Gammaproteobacteria. *I*: Relative fecal mRNA expression of BCoAT and FTHFS in WT and KO mice fed an NC diet and an HFD. NC diet–fed mice, $n = 8$ per group. HFD-fed WT mice, $n = 9$; HFD-fed KO mice, $n = 6$. Data are reported as the mean ± SEM. *$P < 0.05$.
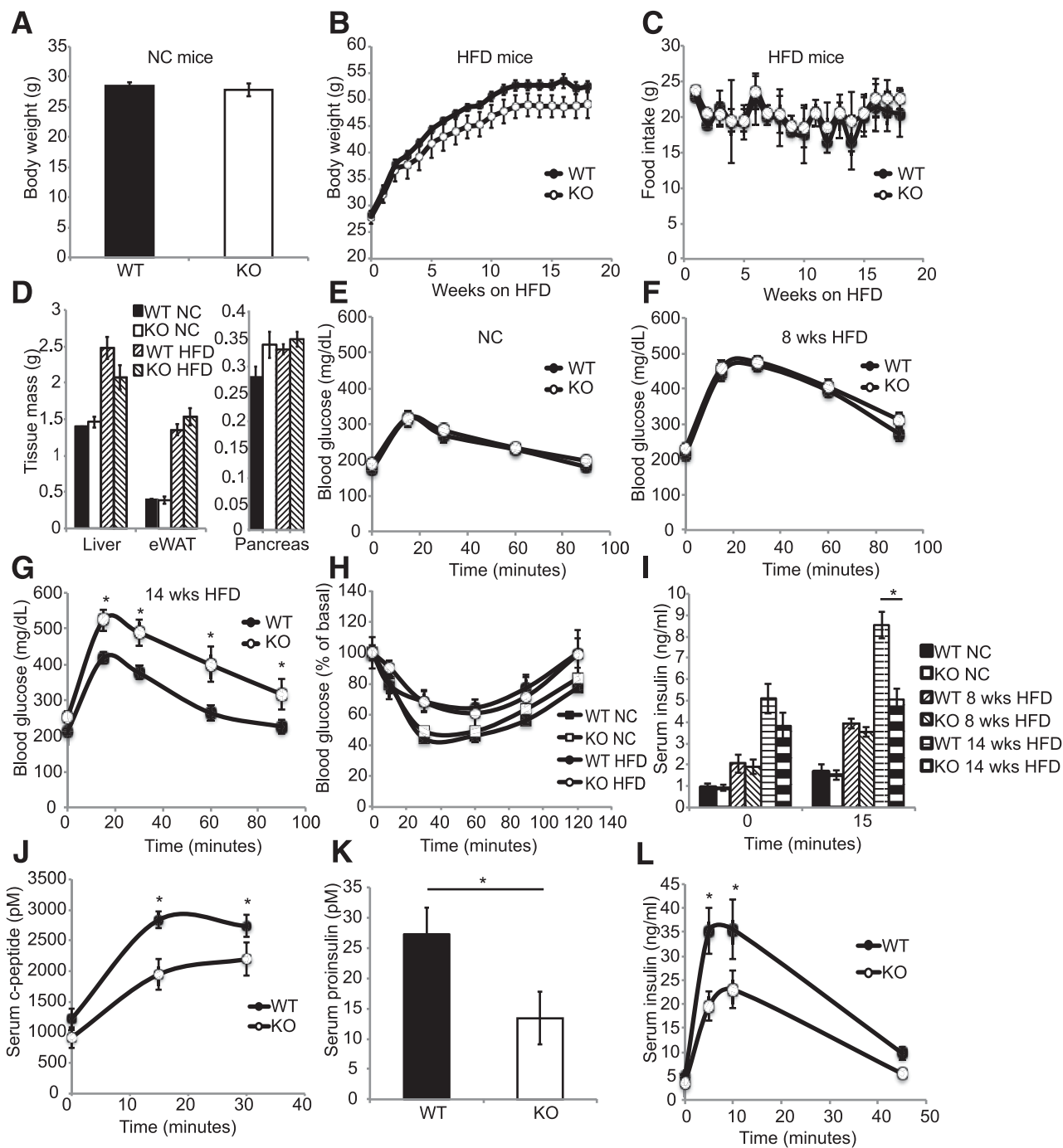
Figure 2—GPR43 KO mice exhibit impaired glucose tolerance and insulin secretion. *A*: Body weight of NC diet–fed WT and KO mice, *n* = 10 per group. *B*: Body weight of HFD-fed WT and KO mice. WT mice, *n* = 9; KO mice, *n* = 7. Data are reported as the mean ± SEM. *C*: Food intake of HFD-fed WT and KO mice. WT mice, *n* = 4; KO mice, *n* = 4. *D*: Tissue weight of WT and KO mice fed an NC diet and an HFD. Data are reported as the mean ± SEM, *n* = 7–10. Intraperitoneal GTT (1 g/kg) in mice fed an NC diet (*E*; mean ± SEM, *n* = 10 per group), an 8-week HFD (*F*), and a 14-week HFD (*G*; mean ± SEM; WT, *n* = 9; KO, *n* = 7). *H*: Insulin tolerance test in mice fed an NC diet and a 15-week HFD. Data are reported as the mean ± SEM, *n* = 7–10. *I*: Plasma insulin concentrations during intraperitoneal GTT in mice fed an NC diet, an 8-week HFD, or a 14-week HFD. Data are reported as the mean ± SEM, *n* = 7 per group. Serum C-peptide (*J*) and proinsulin (*K*) levels in mice fed a 14-week HFD during intraperitoneal GTT. Data are reported as the mean ± SEM, *n* = 7 per group. *L*: Serum insulin levels of mice fed a 14-week HFD during arginine tolerance test. Data are reported as the mean ± SEM, *n* = 6–7 per group. *P < 0.05. eWAT, epididymal white adipose tissue.

insulin sensitivity (Fig. 2*H*) compared with WT mice. In contrast, after prolonged HFD feeding (14 weeks), KO mice developed fasting hyperglycemia and glucose intolerance (Fig. 2*G*), despite a normal hypoglycemic response to insulin (Fig. 2*H*), suggesting a defect in insulin secretion. Consistent with this, KO mice fed an HFD for 14 weeks

showed significantly lower post–glucose challenge serum insulin (Fig. 2*I*), proinsulin (Fig. 2*K*), and C-peptide (Fig. 2*J*) levels, compared with their WT counterparts, while no difference was observed between genotypes in mice fed an NC diet or an 8-week HFD (Fig. 2*I*). Consistent with a generalized insulin secretion defect, KO mice also exhibited significantly lower serum insulin levels after arginine stimulation (Fig. 2*L*).

To examine whether the KO phenotype was due to a β-cell defect, we assessed glucose-stimulated insulin secretion (GSIS) of isolated islets. There was no difference in GSIS between WT and KO islets from mice fed an NC diet (Fig. 3*A*). As expected, insulin secretion was greater in islets from HFD-fed mice. However, under high-glucose conditions (16.7 mmol/L) islets from HFD-fed KO mice exhibited a marked reduction in GSIS, compared with islets from HFD-fed WT mice (Fig. 3*A*), which is consistent with the relative glucose intolerance exhibited by HFD-fed KO mice during GTTs (Fig. 2*G*). Islets from HFD-fed KO mice also displayed a marked reduction in GLP-1–stimulated insulin secretion (Fig. 3*B*). Together, these results demonstrate that islets from KO mice fed an HFD for 14 weeks have an islet-autonomous insulin secretion defect.

To determine the role of GPR43 activation in insulin secretion, we treated islets with acetate or a selective small-molecule GPR43-specific agonist, PA (referred to as compound 58 in the study by Wang et al. [31]). PA stimulated insulin secretion in islets from WT mice fed both an NC diet (Fig. 3*C*) and a 14-week HFD (Fig. 3*D*), but was without effect in islets from KO mice. Interestingly, acetate had inhibitory effects on insulin secretion in islets from KO mice (Fig. 3*C*), which we postulated was due to the activation of GPR41, which is coupled to Gαi. To examine this further, we used the murine Min6 β-cell line and depleted GPR43, GPR41, or Gαq/11 expression using siRNA (Fig. 3*E*). PA markedly increased GSIS in control cells, but not in GPR43-depleted cells. Similar to our findings in isolated islets, acetate had no effect in control cells, but inhibited insulin secretion in GPR43 knockdown cells (Fig. 3*E*). This inhibitory effect of acetate was absent in GPR41 knockdown cells, again indicating that the inhibitory effect of acetate is mediated via GPR41. siRNA depletion of Gαq/11 blocked the effect of PA on insulin secretion, showing that GPR43 stimulates insulin secretion by coupling to the Gαq/11 pathway. To determine whether long-term exposure to agonists results in desensitization of GPR43, we treated Min6 cells with the agonists for 48 h prior to measuring GSIS. Long-term exposure did not diminish the stimulatory effect of PA on insulin secretion (Fig. 3*F*).

To test the relevance of these findings in humans, we treated human islets with acetate and PA. Consistent with our findings in Min6 cells, PA stimulated insulin secretion (Fig. 3*G*), supporting the potential of GPR43 as a therapeutic target in humans.

GPR43 is coupled to both Gαq and Gαi G-proteins in several cell types. To establish the downstream coupling of

GPR43 in β-cells, we determined whether PLC, the classic target of activated Gαq, is required for GPR43-mediated Min6 insulin secretion. Treatment with the PLC inhibitor U73122 ablated the stimulatory effect of PA, while promoting an inhibitory effect of acetate (Fig. 4*A*), similar to the depletion of GPR43 in Min6 cells (Fig. 3*E*). In contrast, treatment with the Gαi inhibitor pertussis toxin (PTX) had no effect on PA-stimulated insulin secretion (Fig. 4*B*). We next investigated the production of the downstream mediators of Gαq and Gαi signaling, IP$_3$ and cAMP. Consistent with Gαq coupling, PA markedly increased IP$_3$ generation (measured by the accumulation of the metabolite IP$_1$) (Fig. 4*C*), but had no effect on forskolin-stimulated cAMP production (Fig. 4*D*).

We also performed experiments with the rat-derived Ins-1 cell line. Unexpectedly, GPR43 activation in Ins-1 cells inhibited insulin secretion (Fig. 4*E*). Treatment with U73122 and PTX revealed that the inhibitory effect of PA was due to Gi signaling (Fig. 4*E* and *F*). Consistent with this, PA inhibited cAMP production but did not induce IP$_3$ production (Fig. 4*G* and *H*). Therefore, GPR43 is primarily coupled to Gαq in Min6 cells, whereas it is coupled to Gαi in Ins-1 cells.

We then examined GPR43 signaling in murine and human islets. Since mice on a prolonged HFD (14 weeks) exhibit a dramatic defect in insulin secretion, which is not present in mice on an NC diet or a short-term HFD, we examined IP$_3$ and cAMP production in islets from all conditions. PA stimulated IP$_3$ production in all groups, but this effect was much greater in islets from mice fed an HFD for 14 weeks (Fig. 4*I*). In contrast, PA inhibited forskolin-stimulated cAMP production to a comparable extent in all three groups (Fig. 4*J*). This shows that GPR43 is coupled to both Gαq and Gαi in murine islets, and that the ratio of stimulatory (IP$_3$) to inhibitory (inhibition of cAMP) signals increases with HFD. As in murine islets from mice fed an HFD, PA stimulated inhibited cAMP production and robustly increased IP$_3$ production (Fig. 4*K* and *L*) in human islets.

IP$_3$ increases insulin secretion by stimulating the release of calcium from the endoplasmic reticulum. In line with this, PA increased cytosolic calcium concentrations in Min6 cells (Fig. 4*M*). Taken together, these findings demonstrate that GPR43 activation in murine and human islets potentiates insulin secretion via coupling to Gαq, activation of PLC, production of IP$_3$, and increased intracellular calcium concentrations.

Tolhurst et al. (29) have previously demonstrated that SCFAs signal via GPR43 to stimulate GLP-1 secretion from intestinal enteroendocrine cells. We, therefore, performed an oral GTT in mice fed an HFD for 16 weeks, and assessed serum glucose, insulin, and gut hormone levels. As with the intraperitoneal glucose studies (Fig. 2), the KO mice exhibited elevated blood glucose and lower insulin secretion (Fig. 5*A* and *B*). In line with previous studies, KO mice displayed decreased levels of GLP-1, GIP, and PYY secretion (Fig. 5*C–E*).
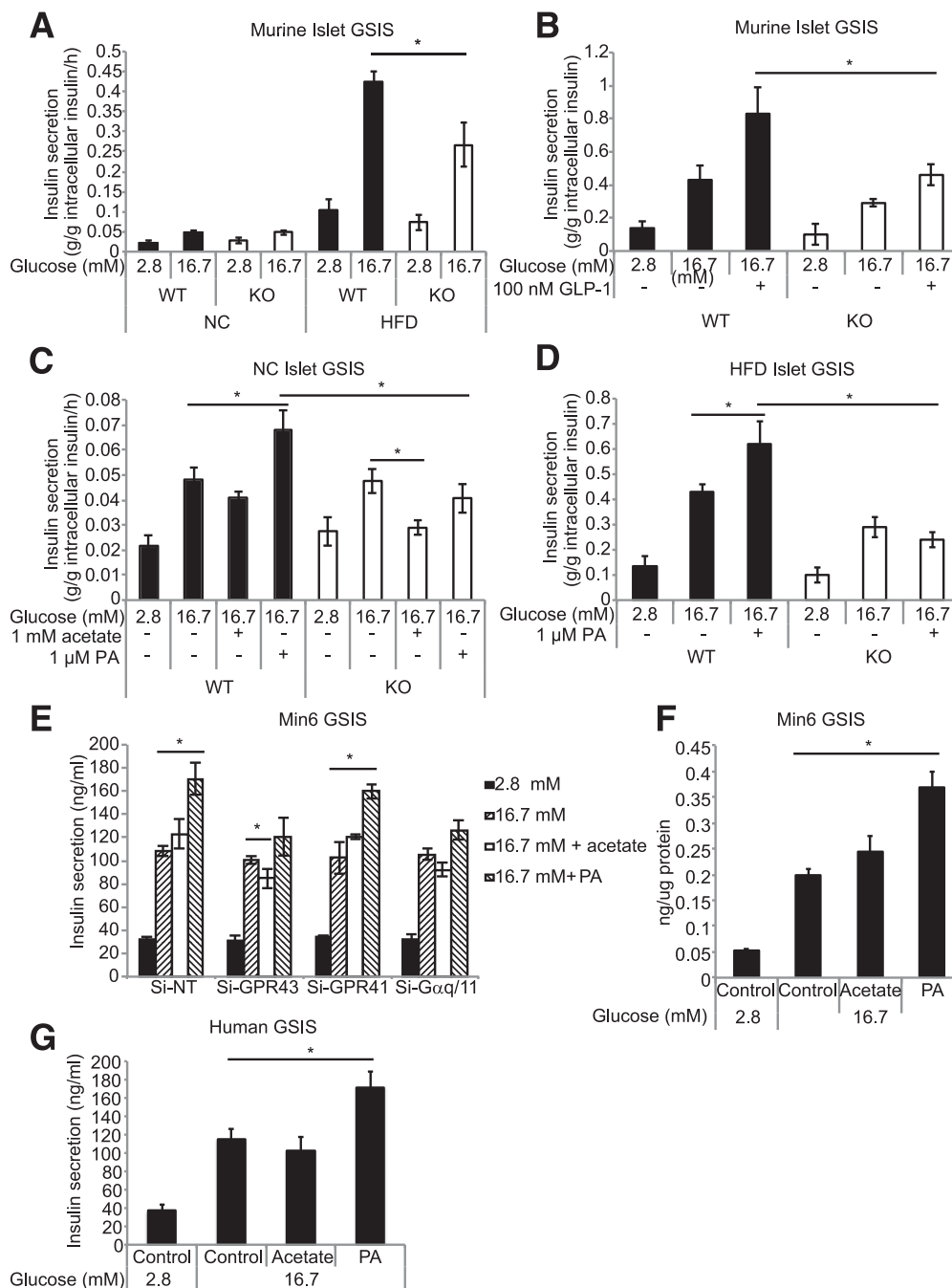
Figure 3—Islets from HFD-fed GPR43-deficient mice display reduced insulin secretion, and GPR43 agonists potentiate insulin secretion. *A*: Glucose-stimulated insulin secretion from isolated islets of WT and KO mice fed an NC diet and a 14-week HFD. Data are reported as the mean ± SEM of three independent experiments. *B*: Glucose- and GLP-1–stimulated insulin secretion from isolated islets of HFD-fed WT and KO mice. Data are reported as the mean ± SEM, *n* = 6 per group. Glucose-stimulated insulin secretion of primary isolated islets from NC diet–fed (*C*) and 14-week HFD-fed (*D*) WT and KO mice in the presence of 1 mmol/L acetate or 1 μmol/L PA. Data are reported as the mean ± SEM of three independent experiments. *E*: GSIS in GPR43, GPR41, or Gαq/11 siRNA-depleted Min6 cells. Data are reported as the mean ± SEM. *F*: GSIS in Min6 cells treated with 1 mmol/L acetate or 1 μmol/L PA for 48 h. *G*: GSIS in isolated human islets in the presence of 1 mmol/L acetate or 1 μmol/L PA. Data are reported as the mean ± SEM, *n* = 3. *P < 0.05.

HFD-induced β-cell compensation involves increased β-cell mass in addition to increased β-cell function. Immunohistological studies showed no difference in β-cell mass between islets of WT and KO mice fed an NC diet (Fig. 6*A*), suggesting that GPR43 does not affect β-cell development. As expected, β-cell mass increased in WT mice fed an HFD compared with WT mice fed an NC diet, but did not increase in KO mice fed an HFD (Fig. 6*A*), resulting in relatively reduced β-cell mass in KO mice after being fed an HFD for 14 weeks. This is due to the
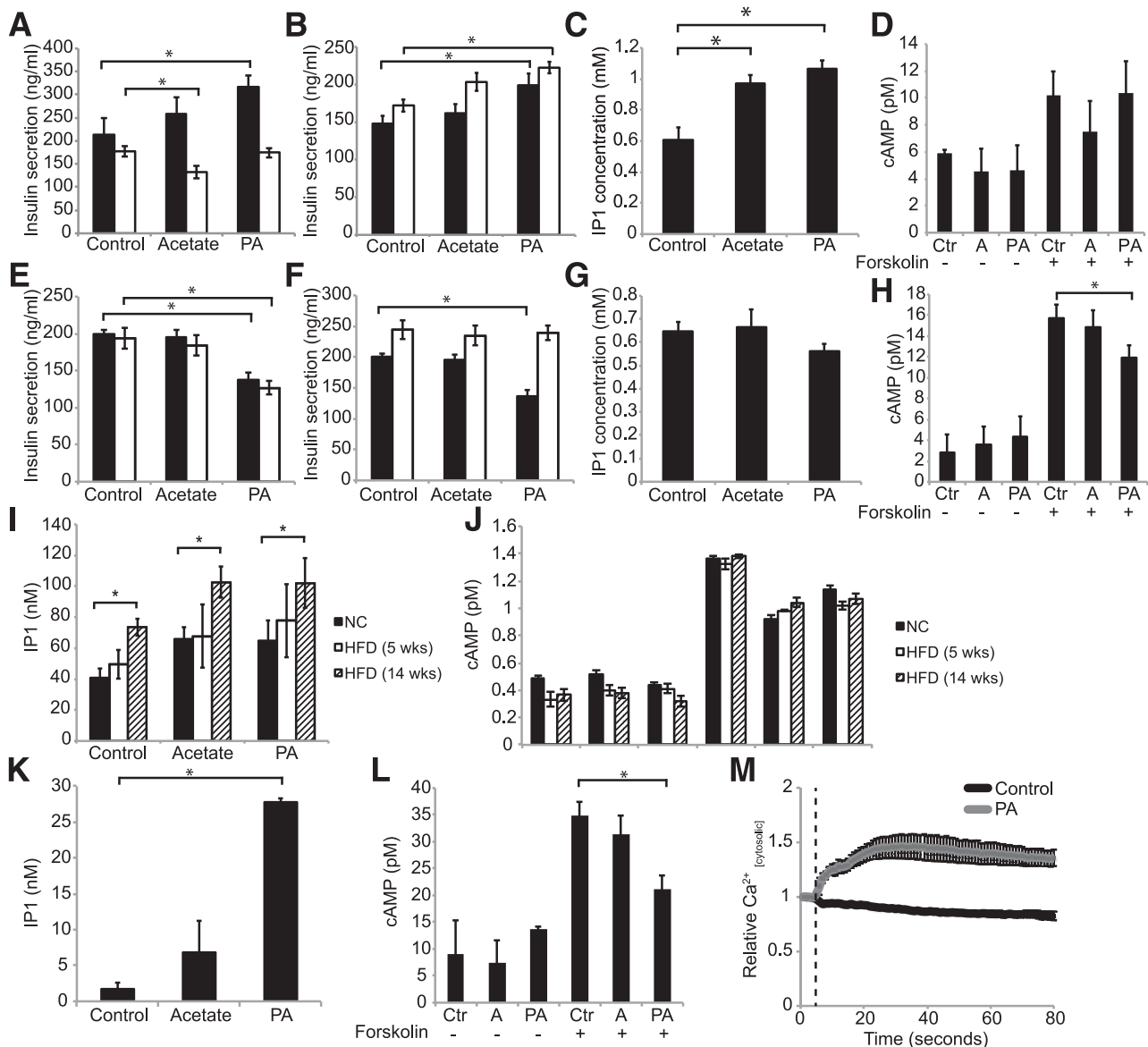
Figure 4—GPR43-stimulated insulin secretion is dependent on PLC. *A*: Min6 GSIS in the presence of PLC inhibitor. Black bars, control; white bars, PLC inhibitor. *B*: Min6 GSIS in the presence of PTX. Black bars, control; white bars, PTX. *C*: IP$_1$ generation in Min6 cells treated with 1 mmol/L acetate or 1 μmol/L PA. *D*: Forskolin-stimulated cAMP production in Min6 cells. Data are reported as the mean ± SEM of three independent experiments. *E*: Ins-1 GSIS in the presence of PLC inhibitor. Black bars, control; white bars, PLC inhibitor. *F*: Ins-1 GSIS in the presence of PTX. Black bars, control; white bars, PTX. *G*: IP$_1$ generation in Ins-1 cells treated with 1 mmol/L acetate or 1 μmol/L PA. *H*: Forskolin-stimulated cAMP production in Ins-1 cells. Data are reported as the mean ± SEM of three independent experiments. *I*: IP$_1$ production isolated islets from mice fed an NC diet, a 5-week HFD, and a 14-week HFD. *J*: Forskolin-stimulated cAMP production in isolated islets from mice fed an NC diet, a 5-week HFD, and a 14-week HFD. Data are reported as the mean ± SEM, n = 4–5 per group. *K*: IP$_1$ production in human islets. *L*: Forskolin-stimulated cAMP production in human islets. Data are reported as the mean ± SEM, n = 3. *M*: Cytosolic calcium in Min6 cells treated with 1 μmol/L PA. Dashed vertical line indicates the addition of DMSO (control) or PA. Data are reported as the mean ± SEM of three independent experiments. *P < 0.05. A, acetate; Ctr, control.

combined effects of reduced islet size (Fig. 6*B*) and reduced islet number (Fig. 6*C*), and is consistent with reduced pancreatic insulin content in KO mice (Fig. 6*D*). The morphologic features of the islets from WT and KO mice, such as the predominance of Ins$^+$ β-cells in the core surrounded by glucagon-positive α-cells, were comparable (Fig. 6*E*). These findings suggest that the in vivo phenotype is due to both reduced β-cell mass and reduced β-cell function.

To determine whether the reduced β-cell mass in the KO mice was due to decreased proliferation, BrdU was administered for 4 weeks in the drinking water of WT and KO mice during HFD feeding (weeks 8–12 of the HFD). We quantified the number of Ins$^+$ β-cells per islet and the number of BrdU$^+$ β-cells (BrdU$^+$/Ins$^+$), to calculate the percentage of β-cells that had undergone proliferation (BrdU$^+$Ins$^+$/Ins$^+$). The percentage of BrdU$^+$ β-cells
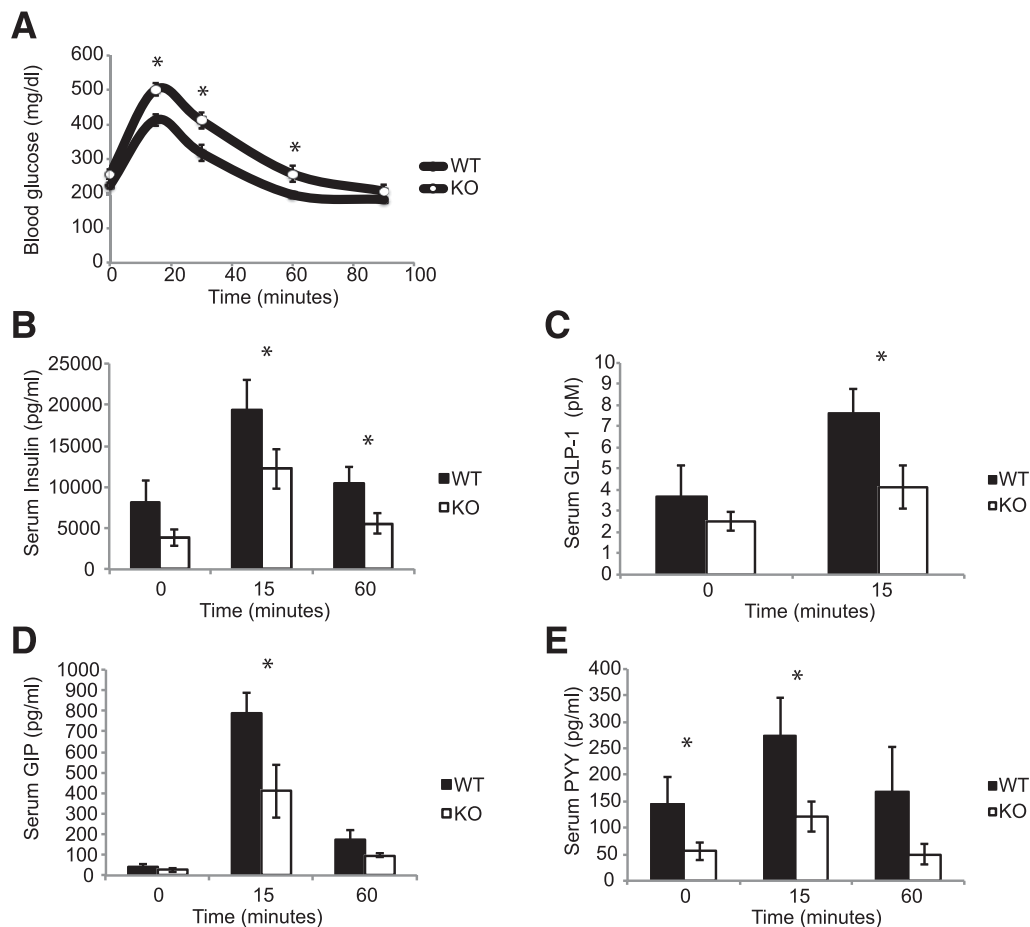
Figure 5—GPR43 KO mice have reduced serum gut peptide concentrations. *A*: Blood glucose values during oral GTT. Serum gut peptides were measured at baseline, and at 15 and 60 min during an oral GTT. Insulin (*B*), active GLP-1 (*C*), GIP (*D*), and PYY (*E*). Data are reported as the mean ± SEM, *n* = 6–7 per group. *$P < 0.05$.

was significantly higher in islets from WT mice compared with islets from KO mice (Fig. 6*F* and *G*), indicating reduced β-cell proliferation in KO mice. To confirm this in vitro, we performed proliferation assays in Min6 cells and thymidine incorporation studies with isolated islets. Treatment of Min6 cells with acetate or PA increased β-cell proliferation in control cells, with an effect comparable to that of exendin-4 (Fig. 6*H*), but was without effect in GPR43- or Gαq/11-depleted cells. Similarly, treatment of isolated islets with acetate or PA for 48 h significantly increased thymidine incorporation into islets (Fig. 6*I*). To assess any contribution of β-cell apoptosis to the reduced β-cell mass in the islets of KO mice, we stimulated Min6 apoptosis with palmitate in the presence or absence of acetate or PA. Both agonists failed to reduce palmitate-induced Min6 cell apoptosis (Fig. 6*J*). Thus, these studies demonstrate that GPR43 activation increases β-cell mass by a direct effect on β-cell proliferation.

The maintenance of functional β-cell mass, including insulin transcription, is regulated by a number of key β-cell transcription factors, including PDX-1, NeuroD,

and MafA. Islets from KO mice fed an HFD for 14 weeks display a lower expression of mRNA-encoding β-cell transcription factors and insulin compared with islets from WT mice (Fig. 7*B*), while no difference was observed in islets from NC-fed mice (Fig. 7*A*). Consistent with this, islets from KO mice fed an HFD display reduced insulin protein content compared with islets from WT mice (Fig. 7*C*).

To determine whether GPR43 agonists can directly regulate β-cell gene expression, we treated Min6 cells with acetate or PA. Treatment with either agonist for 48 h induced the expression of insulin, PDX-1, and NeuroD in Min6 cells (Fig. 7*D–I*). GPR43 activation has been shown to activate extracellular signal–related kinase signaling in neutrophils and adipocytes. To determine whether Gαq, GαI, or extracellular signal–related kinase signaling mediate GPR43-induced gene expression, we depleted Gαq/11 with siRNA or treated cells with PTX or an inhibitor of mitogen-activated protein kinase/extracellular signal–related kinase kinase (MEK) (PD98059). The induction of insulin, PDX-1, and NeuroD by acetate and PA is dependent on Gαq/11 and MEK signaling (Fig. 7*D–I*), but not on GαI signaling (Fig. 7*J–L*).
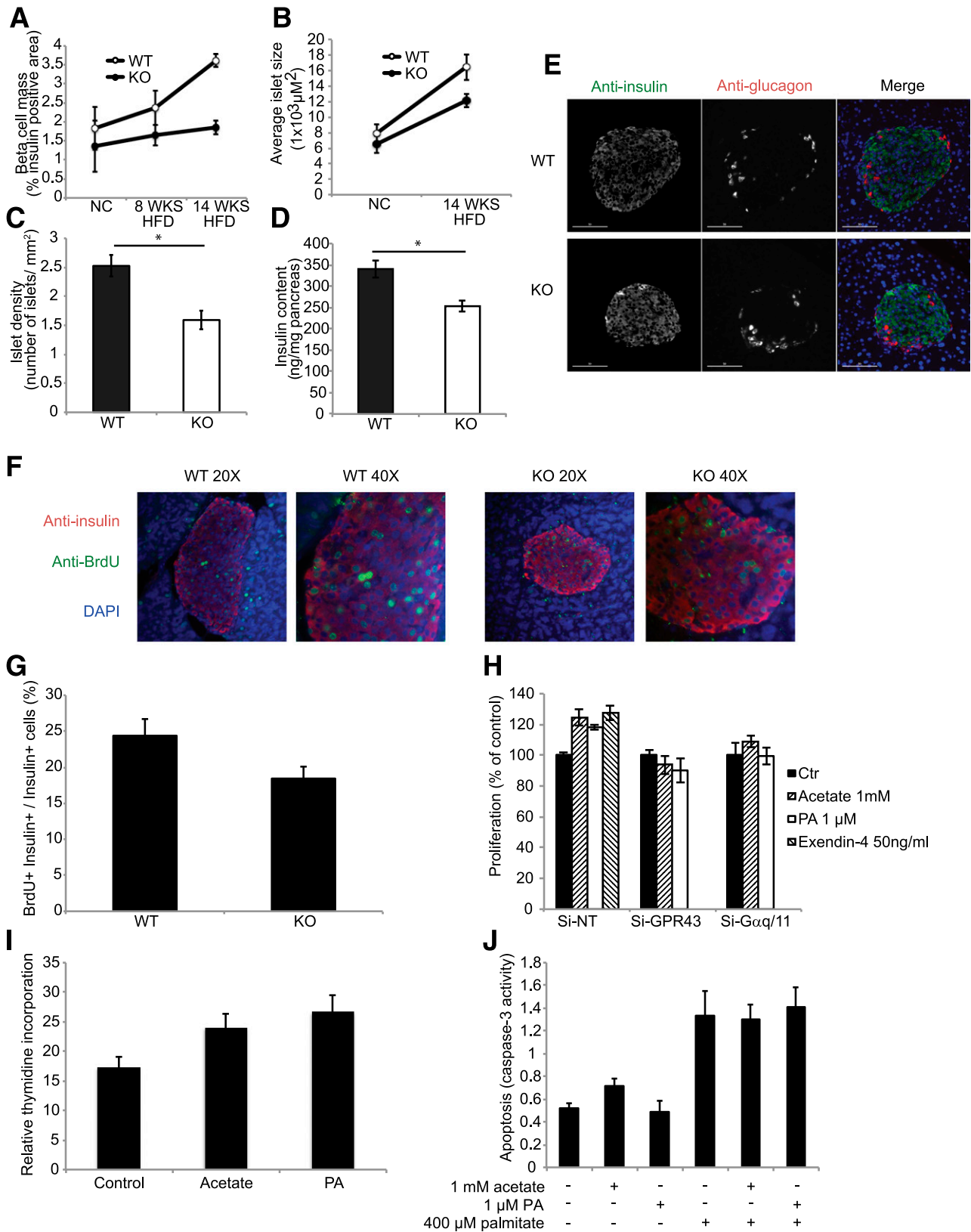
Figure 6—GPR43 regulates β-cell proliferation and mass. *A*: β-cell mass, measured as the percentage of the insulin-immunopositive area in pancreatic sections from WT and KO mice fed an NC diet, an 8-week HFD, and a 14-week HFD. *B*: Average islet size, determined by immunofluorescence, in pancreatic sections from WT and KO mice fed an NC diet and an HFD. *C*: Islet density, measured as the number of islets per square millimeter of pancreas area in HFD-fed WT and KO mice. *D*: Insulin content of HFD-fed WT and KO pancreata. Data are reported as the mean ± SEM. *P < 0.05, WT vs. KO. *E*: Immunohistochemistry analysis of the islet architecture of HFD-fed WT and KO mice. Anti-insulin is shown in green, and anti-glucagon is shown in red. *F*: Pancreatic sections stained for anti-insulin are shown in red, for

Previous reports have identified GPR43 as a modulator of inflammation, particularly in the intestinal mucosa. As obesity causes inflammation, which contributes to insulin resistance, we assessed inflammation in metabolic tissues of WT and KO mice. We observed no differences in inflammatory gene expression in epididymal adipose tissue or liver between WT and KO mice (Fig. 8A and B). We also saw no differences in HFD-induced hepatic steatosis, as assessed by hematoxylin-eosin and Oil Red O staining (Fig. 8C), or hepatic gluconeogenic gene expression (Fig. 8D) between WT and KO mice.

We also performed bone marrow transplant studies, reconstituting irradiated WT mice with WT or KO bone marrow. To confirm the successful generation of chimeric mice, we analyzing GPR43 mRNA expression in peripheral white blood cells (Fig. 8E) to show GPR43 gene deletion. We did not observe any differences in weight gain, glucose or insulin tolerance, insulin secretion, or fasting free fatty acid levels (Fig. 8F–J) between WT and KO mice, confirming that GPR43 on immune cells does not contribute to glucose tolerance.

DISCUSSION

The etiology of T2D involves both insulin resistance and relative β-cell failure, and insulin-resistant patients who maintain compensatory hyperinsulinemia generally avoid frank hyperglycemia (3,5). Here we show that the SCFA/GPR43 system can regulate the process of β-cell compensation in the insulin-resistant state. Thus, GPR43 KO mice are unaffected on an NC diet but develop marked glucose intolerance on an HFD due to reduced insulin secretion. Our studies with isolated islets and Min6 cells show that this phenotype is a β-cell–autonomous defect. GPR43 activation potentiates glucose-, arginine-, and GLP-1–stimulated insulin secretion in vivo, and from isolated murine and human islets, and Min6 cells. Taken together, these studies suggest that GPR43 is a potential therapeutic target for the treatment of T2D.

Our in vitro studies show that, in the presence of glucose, GPR43 activation stimulates insulin secretion by a Gαq/11- and PLC-dependent mechanism. Gαq signaling is known to play a key role in regulating β-cell insulin secretion via PLC-mediated production of diacylglycerol and IP$_3$ (35–38). IP$_3$ subsequently induces insulin secretion by stimulating the release of endoplasmic reticulum calcium to the cytosol (38). Consistent with the activation of this pathway, GPR43 agonists stimulate PLC, IP$_3$

generation, and intracellular calcium mobilization. Interestingly, we show that the coupling of GPR43 is distinct in different cell lines. In isolated murine and human islets, GPR43 is coupled to both Gαq and Gαi, as indicated by the concurrent stimulation of IP$_3$ and inhibition of cAMP production by GPR43 agonists. However, the net balance of these pathways is stimulatory, resulting in the potentiation of insulin secretion. Similarly, GPR43 is predominately coupled to Gαq in Min6 cells, but to Gαi in Ins-1 cells. It is unclear whether this is due to species differences or another unknown factor. Nonetheless, together our data show that GPR43 has the capacity to couple to both pathways and suggest that agonists biased toward Gαq signaling could be clinically effective.

Our findings clearly demonstrate that GPR43 has effects to potentiate nutrient-induced insulin secretion, but also suggest that GPR43 may have more long-term effects on β-cell function and mass. For instance, we observed that islets from HFD-fed KO mice display reduced expression of several transcription factors that are critical for maintaining normal β-cell function (39–41). Our in vitro data with Min6 cells show that the expression of these genes is regulated by GPR43 activation in a cell-autonomous manner. Of particular interest, PDX-1, MafA, and NeuroD1 work in concert to regulate insulin gene transcription and exocytosis, and their expression is reduced in diabetic states (42–44). Consistent with this, we observed reduced insulin mRNA and protein expression along with reduced GSIS in isolated islets from KO mice. Together, this suggests that KO islets are less functional, at least in part, owing to the lack of chronic GPR43 activation with reduced gene expression.

GPR43 KO animals fail to appropriately expand β-cell mass in response to HFD feeding, owing to reduced β-cell proliferation. GPR43 agonists increase Min6 proliferation in a GPR43- and Gαq/11-dependent manner. Of note, long-term pharmacological activation of β-cell Gαq signaling, independent of endogenous Gαq/11 receptors, has shown that Gαq signaling regulates β-cell mass and function in mice through the induction of several genes critical for β-cell health and proliferation (37). Our finding that GPR43 stimulates the proliferation of isolated islets and Min6 cells indicates that this is a β-cell–autonomous effect and is not a consequence of hyperglycemia or GLP-1 levels in vivo. Further studies are needed to determine whether this phenomenon translates to human islets.

---

anti-BrdU are shown in green, and for DAPI are shown in blue. G: Proliferation of β-cells, quantified as the number of nuclei from BrdU$^+$ Ins$^+$ cells, divided by the number of nuclei from Ins$^+$ cells, multiplied by 100. H: Proliferation of Min6 cells depleted of GPR43 or Gαq/11 by siRNA, in the presence of 1 mmol/L acetate, 1 μmol/L PA, or 50 ng/mL exendin-4. I: Thymidine incorporation into isolated islets from WT mice in the presence of acetate or PA for 48 h, normalized to total protein content. J: Palmitate (400 μmol/L) induced apoptosis of Min6 cells, in the presence of 1 mmol/L acetate or 1 μmol/L PA. Data are reported as the mean ± SEM of three independent experiments. *P < 0.05, treatment vs. control. Ctr, control.
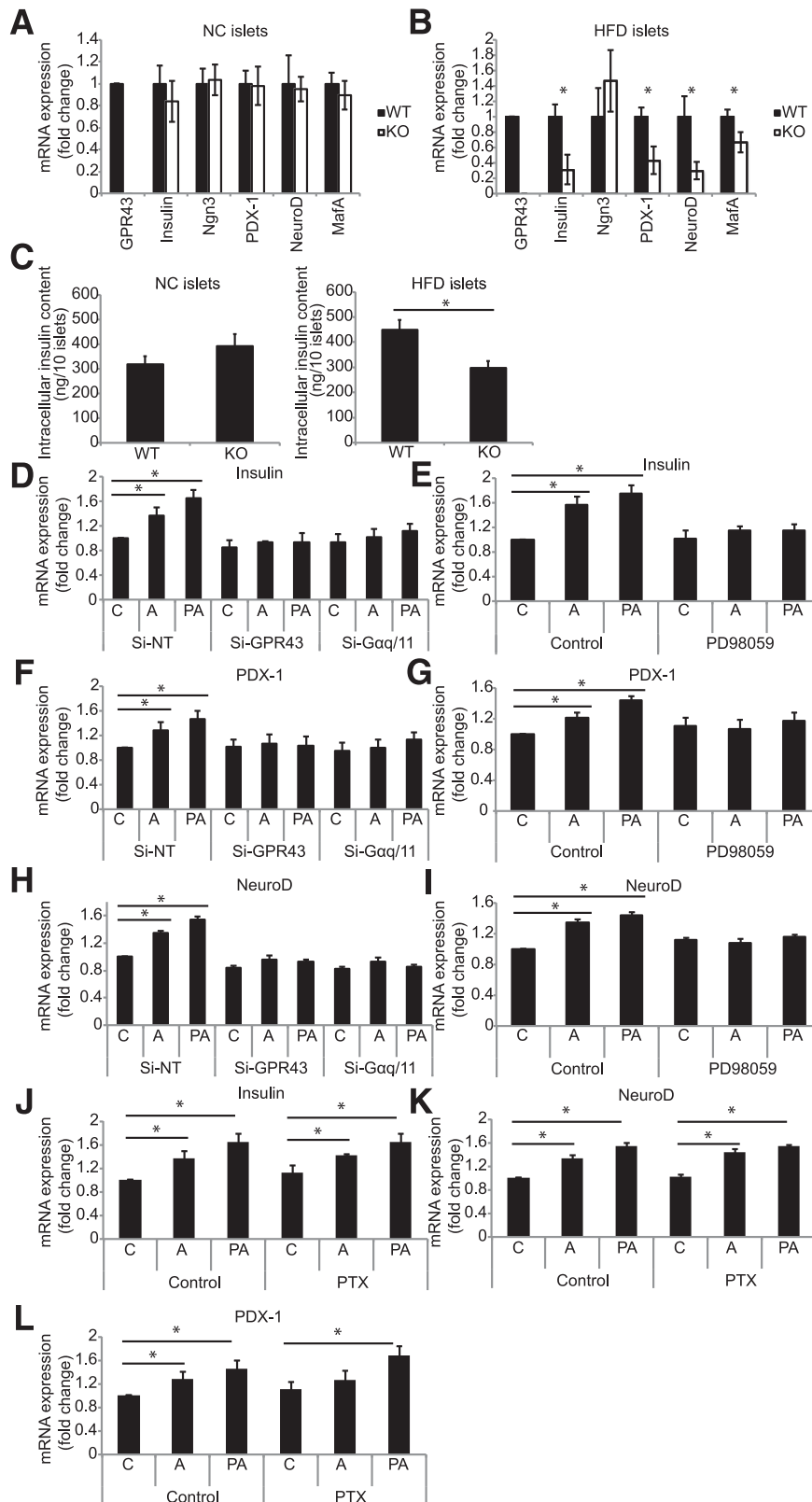
Figure 7—GPR43 regulates expression of key β-cell genes. mRNA expression of β-cell genes in isolated islets from WT and KO mice fed an NC diet (A) and a 14-week HFD (B). Data are reported as the mean ± SEM, n = 6–8 per group. C: Intracellular insulin content of islets from WT and KO mice fed an NC diet (left panel) and an HFD (right panel). Data are reported as the mean ± SEM. D–I: The mRNA expression of β-cell genes in Min6 cells treated with acetate (1 mmol/L) or PA (1 μmol/L). A, acetate; C, control. D, F, and H: Min6 cells depleted of GPR43 or Gαq/11 by siRNA. E, G, and I: Min6 cells treated with MEK inhibitor (PD98059). Data are reported as the mean ± SEM of three independent experiments. J–L: The mRNA expression of β-cell genes in Min6 cells treated with PTX. Data are reported as the mean ± SEM of three independent experiments. *P < 0.05, treatment vs. control.
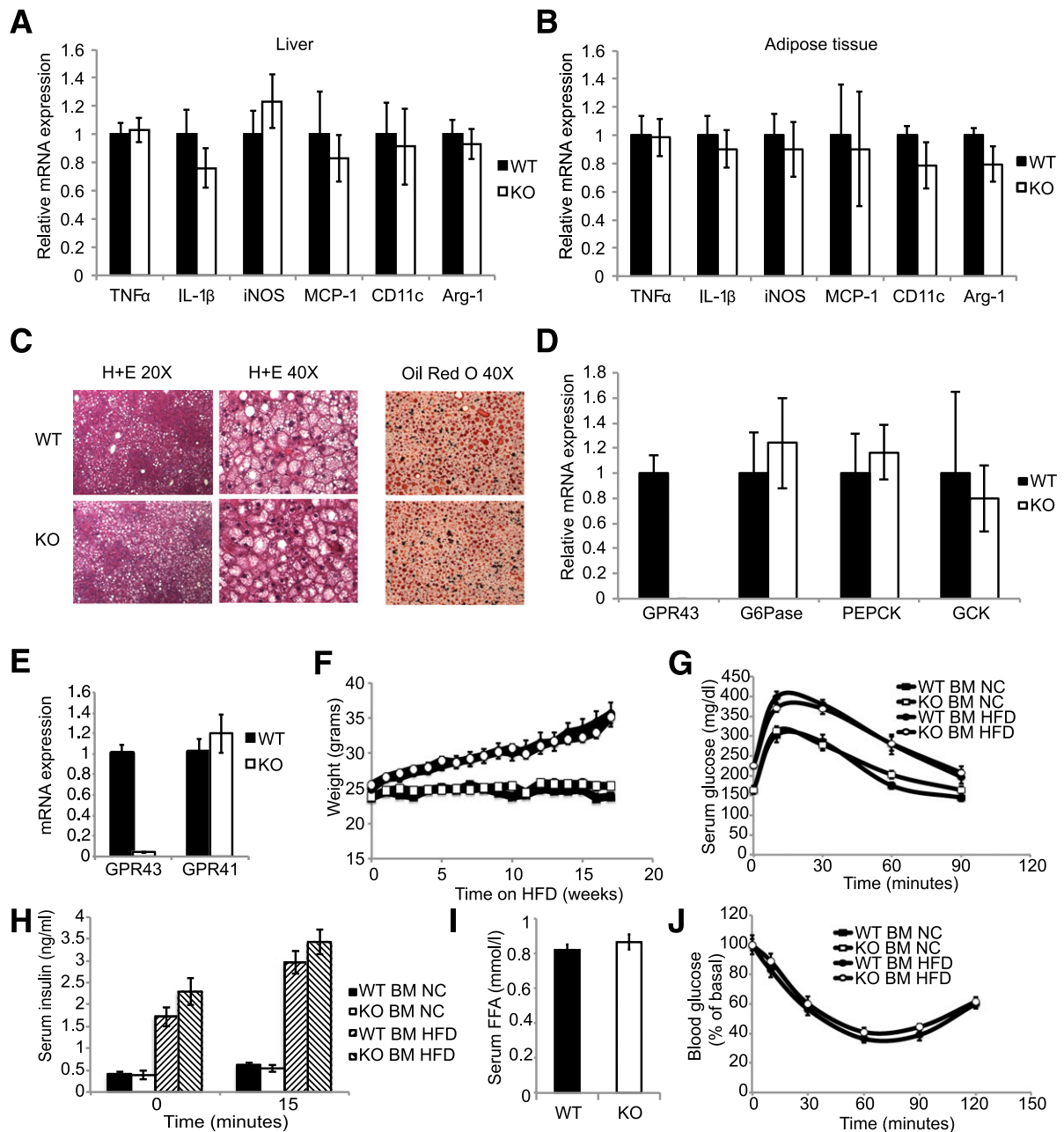
Figure 8—Inflammation does not contribute to the KO phenotype. mRNA expression of pro/anti-inflammatory genes in liver (*A*) and eWAT (*B*) of WT and KO HFD-fed mice. Data are reported as the mean ± SEM, *n* = 5 per group. *C*: Hematoxylin-eosin (H+E) staining and Oil Red O staining of hepatic sections from HFD-fed WT and KO mice. *D*: mRNA expression of hepatic gluconeogenic genes in HFD-fed WT and KO mice. *E–J*: Hematopoietic cells from GPR43-deficient mice were generated by bone marrow transplantation. *E*: mRNA expression of GPR43 and GPR41 in white blood cells of reconstituted mice. Data are reported as the mean ± SEM, *n* = 4 per group. *F*: Body weight of NC-diet–fed and HFD-fed reconstituted mice. Data are reported as the mean ± SEM, *n* = 10–12 per group. *G*: Intraperitoneal GTT. Data are reported as the mean ± SEM, *n* = 10–12 per group. *H*: Serum insulin concentrations during intraperitoneal GTT. Data are reported as the mean ± SEM, *n* = 6 per group. *I*: Fasting serum free fatty acid concentrations. *J*: Insulin tolerance test, *n* = 10 per group. Data are reported as the mean ± SEM. BM, bone marrow; FFA, free fatty acid; GCK, glucokinase gene; IL-1β, interleukin-1β; iNOS, inducible nitric oxide synthase; TNFα, tumor necrosis factor-α.

Our data show that the function of GPR41, which is also activated by acetate, opposes that of GPR43, inhibiting insulin secretion. Thus, acetate does not have a net effect on insulin secretion in Min6 cells or isolated WT islets unless GPR43 is depleted, whereas a GPR43-specific agonist potentiates insulin secretion. GPR41 KO

studies are needed to show whether GPR41 antagonists would also be useful for the treatment of diabetes.

An interesting aspect of the phenotype is that KO mice do not develop marked glucose intolerance until 14 weeks of HFD feeding. We hypothesize that this is due to the complex combined effects of several contributing

factors. First, we show that GPR43-mediated production of IP$_3$ is greater in islets from mice fed an HFD for 14 weeks, compared with those from mice fed an NC diet or a short-term HFD, while GPR43-mediated inhibition of cAMP is comparable across all groups. These data indicate that with extended HFD feeding, GPR43 coupling to the Gαq signaling pathway becomes more dominant, leading to the phenotype of increased GPR43-stimulated GSIS. Importantly, this phenotype of robust Gαq coupling and IP$_3$ generation is maintained in human islets. Second, GPR43 regulates compensatory changes in β-cell mass and gene expression in response to hyperglycemia and hyperinsulinemia. In our studies, a deficit in β-cell mass in KO mice takes 14 weeks to emerge, indicating that GPR43 can modulate β-cell mass and differentiation in the chronic insulin-resistant state. Finally, the expression of GPR43 and the serum level of acetate increase with HFD feeding, possibly owing to changes in microbiota composition.

Several studies have shown a role for GPR43, and the regulation of intestinal homeostasis and inflammation, but the metabolic functions of GPR43 are still unclear. Tolhurst et al. (29) showed that GPR43 KO mice demonstrate decreased glucose tolerance, reduced insulin secretion, and impaired GPR43- and Gαq-mediated GLP-1 secretion, with no change in body weight on an NC diet. Consistent with this, we observed decreased glucose tolerance, decreased insulin levels, and reduced incretin levels in HFD KO versus WT mice. Bjursell et al. (45) found decreased insulin secretion without a change in glucose levels in HFD GPR43 KO mice, which is generally consistent with our results, except that these workers observed decreased weight gain in KO mice. Finally, when Kimura et al. (21) studied GPR43 KO mice on an HFD, they showed a marked increase in adiposity accompanied by glucose intolerance and elevated insulin levels. We observed none of these differences, including no changes in adipose tissue and liver inflammation or insulin sensitivity. Each of these studies was performed in a different mouse strain, under different experimental circumstances, and in the prior studies there is no information on relative coupling of GPR43 into Gαq versus Gαi signaling pathways.

It is widely suggested that gastrointestinal microbiota dysbiosis can influence the development of obesity, insulin resistance, and diabetes (8–10). We propose that the SCFA/GPR43 axis can be a link between the microbiota and metabolic function of the host. Thus, β-cell expression of GPR43 and the circulating concentrations of acetate are increased in HFD-fed mice. This is in line with the finding (10) that obese humans have higher fecal SCFA concentrations compared with their lean counterparts, suggesting a physiological role for the coupling of microbial products to insulin secretion. We propose that GPR43 may act as a sensor for nutrient availability that promotes energy storage through insulin secretion. In times of energy excess, such as obesity, the composition of the microbiota may adapt to produce more SCFAs that work through GPR43 to potentiate insulin secretion and β-cell health.

Taken together, our findings describe a novel pathway regulating β-cell function. GPR43-deficient mice display glucose intolerance due to reduced β-cell function and mass, mimicking the T2D state. GPR43 activation promotes β-cell insulin secretion, β-cell proliferation, and the expression of β-cell differentiation genes. Our agonist studies are limited to in vitro experiments owing to the lack of a selective GPR43 agonist suitable for in vivo experiments. Thus, future in vivo studies are needed to confirm the effectiveness of GPR43 as a treatment for diabetes. However, our in vitro findings and the severe defect in insulin secretion observed in KO mice together suggest that GPR43 is an attractive target for future studies. It is possible that small-molecule agonists of GPR43 could emerge as a useful tool to treat β-cell dysfunction in T2D.

References

1. Leahy JL. Pathogenesis of type 2 diabetes mellitus. Arch Med Res 2005;36:197–209
2. Camastra S, Manco M, Mari A, et al. β-Cell function in morbidly obese subjects during free living: long-term effects of weight loss. Diabetes 2005;54:2382–2389
3. Weyer C, Bogardus C, Mott DM, Pratley RE. The natural history of insulin secretory dysfunction and insulin resistance in the pathogenesis of type 2 diabetes mellitus. J Clin Invest 1999;104:787–794
4. Bonner-Weir S, Li W-C, Ouziel-Yahalom L, Guo L, Weir GC, Sharma A. β-Cell growth and regeneration: replication is only part of the story. Diabetes 2010;59:2340–2348
5. Butler AE, Janson J, Bonner-Weir S, Ritzel R, Rizza RA, Butler PC. β-Cell deficit and increased β-cell apoptosis in humans with type 2 diabetes. Diabetes 2003;52:102–110
6. Talchai C, Xuan S, Lin HV, Sussel L, Accili D. Pancreatic β cell dedifferentiation as a mechanism of diabetic β cell failure. Cell 2012;150:1223–1234
7. Ahrén J, Ahrén B, Wierup N. Increased β-cell volume in mice fed a high-fat diet: a dynamic study over 12 months. Islets 2010;2:353–356
8. Karlsson FH, Tremaroli V, Nookaew I, et al. Gut metagenome in European women with normal, impaired and diabetic glucose control. Nature 2013;498:99–103
9. Turnbaugh PJ, Ley RE, Mahowald MA, Magrini V, Mardis ER, Gordon JI. An obesity-associated gut microbiome with increased capacity for energy harvest. Nature 2006;444:1027–1031
10. Schwiertz A, Taras D, Schäfer K, et al. Microbiota and SCFA in lean and overweight healthy subjects. Obesity (Silver Spring) 2010;18:190–195
11. Larsen N, Vogensen FK, van den Berg FWJ, et al. Gut microbiota in human adults with type 2 diabetes differs from non-diabetic adults. PLoS One 2010;5:e9085

12. Wu X, Ma C, Han L, et al. Molecular characterisation of the faecal microbiota in patients with type II diabetes. Curr Microbiol 2010;61:69–78

13. Cani PD, Bibiloni R, Knauf C, et al. Changes in gut microbiota control metabolic endotoxemia-induced inflammation in high-fat diet–induced obesity and diabetes in mice. Diabetes 2008;57:1470–1481

14. Teixeira TFS, Grześkowiak Ł, Franceschini SCC, Bressan J, Ferreira CLLF, Peluzio MCG. Higher level of faecal SCFA in women correlates with metabolic syndrome risk factors. Br J Nutr 2013;109:914–919

15. Wolever TM, Spadafora P, Eshuis H. Interaction between colonic acetate and propionate in humans. Am J Clin Nutr 1991;53:681–687

16. Vernay M. Origin and utilization of volatile fatty acids and lactate in the rabbit: influence of the faecal excretion pattern. Br J Nutr 1987;57:371–381

17. Stevens CE, Hume ID. Contributions of microbes in vertebrate gastrointestinal tract to production and conservation of nutrients. Physiol Rev 1998;78:393–427

18. Kim MH, Kang SG, Park JH, Yanagisawa M, Kim CH. Short-chain fatty acids activate GPR41 and GPR43 on intestinal epithelial cells to promote inflammatory responses in mice. Gastroenterology 2013;145:396–406.e1–10

19. Maslowski KM, Vieira AT, Ng A, et al. Regulation of inflammatory responses by gut microbiota and chemoattractant receptor GPR43. Nature 2009;461:1282–1286

20. Sina C, Gavrilova O, Förster M, et al. G protein-coupled receptor 43 is essential for neutrophil recruitment during intestinal inflammation. J Immunol 2009;183:7514–7522

21. Kimura I, Ozawa K, Inoue D, et al. The gut microbiota suppresses insulin-mediated fat accumulation via the short-chain fatty acid receptor GPR43. Nat Commun 2013;4:1829

22. Zaibi MS, Stocker CJ, O'Dowd J, et al. Roles of GPR41 and GPR43 in leptin secretory responses of murine adipocytes to short chain fatty acids. FEBS Lett 2010;584:2381–2386

23. Regard JB, Kataoka H, Cano DA, et al. Probing cell type-specific functions of Gi in vivo identifies GPCR regulators of insulin secretion. J Clin Invest 2007;117:4034–4043

24. Ahrén B. Islet G protein-coupled receptors as potential targets for treatment of type 2 diabetes. Nat Rev Drug Discov 2009;8:369–385

25. Leonard JN, Chu ZL, Bruce MA, Boatman PD, inventors; Arena Pharmaceuticals, Inc., assignee. Gpr41 and modulators thereof for the treatment of insulin-related disorders. W.I.P.O. Patent Application WO2006/052566. 11 January 2005

26. Leonard JN, Hakak Y, inventors; Arena Pharmaceuticals, Inc., assignee. Gpr43 and modulators thereof for the treatment of metabolic-related disorders. W.I.P.O. Patent Application WO2006/036688. 21 September 2005

27. Layden BT, Durai V, Newman MV, et al. Regulation of pancreatic islet gene expression in mouse islets by pregnancy. J Endocrinol 2010;207:265–279

28. Hong Y-H, Nishimura Y, Hishikawa D, et al. Acetate and propionate short chain fatty acids stimulate adipogenesis via GPCR43. Endocrinology 2005;146:5092–5099

29. Tolhurst G, Heffron H, Lam YS, et al. Short-chain fatty acids stimulate glucagon-like peptide-1 secretion via the G-protein–coupled receptor FFAR2. Diabetes 2012;61:364–371

30. Ge H, Li X, Weiszmann J, et al. Activation of G protein-coupled receptor 43 in adipocytes leads to inhibition of lipolysis and suppression of plasma free fatty acids. Endocrinology 2008;149:4519–4526

31. Wang Y, Jiao X, Kayser F, et al. The first synthetic agonists of FFA2: discovery and SAR of phenylacetamides as allosteric modulators. Bioorg Med Chem Lett 2010;20:493–498

32. Lee YS, Morinaga H, Kim JJ, et al. The fractalkine/CX3CR1 system regulates β cell function and insulin secretion. Cell 2013;153:413–425

33. Lesniewski LA, Hosch SE, Neels JG, et al. Bone marrow-specific Cap gene deletion protects against high-fat diet-induced insulin resistance. Nat Med 2007;13:455–462

34. Cho I, Yamanishi S, Cox L, et al. Antibiotics in early life alter the murine colonic microbiome and adiposity. Nature 2012;488:621–626

35. Sassmann A, Gier B, Gröne H-J, Drews G, Offermanns S, Wettschureck N. The Gq/G11-mediated signaling pathway is critical for autocrine potentiation of insulin secretion in mice. J Clin Invest 2010;120:2184–2193

36. Winzell MS, Ahrén B. G-protein-coupled receptors and islet function-implications for treatment of type 2 diabetes. Pharmacol Ther 2007;116:437–448

37. Jain S, Ruiz de Azua I, Lu H, White MF, Guettier J-M, Wess J. Chronic activation of a designer G(q)-coupled receptor improves β cell function. J Clin Invest 2013;123:1750–1762

38. Exton JH. Regulation of phosphoinositide phospholipases by hormones, neurotransmitters, and other agonists linked to G proteins. Annu Rev Pharmacol Toxicol 1996;36:481–509

39. Matsuoka T-A, Kaneto H, Miyatsuka T, et al. Regulation of MafA expression in pancreatic β-cells in *db/db* mice with diabetes. Diabetes 2010;59:1709–1720

40. Ohlsson H, Karlsson K, Edlund T. IPF1, a homeodomain-containing transactivator of the insulin gene. EMBO J 1993;12:4251–4259

41. Naya FJ, Huang HP, Qiu Y, et al. Diabetes, defective pancreatic morphogenesis, and abnormal enteroendocrine differentiation in BETA2/neuroD-deficient mice. Genes Dev 1997;11:2323–2334

42. Melloul D, Marshak S, Cerasi E. Regulation of insulin gene transcription. Diabetologia 2002;45:309–326

43. Yang BT, Dayeh TA, Volkov PA, et al. Increased DNA methylation and decreased expression of PDX-1 in pancreatic islets from patients with type 2 diabetes. Mol Endocrinol 2012;26:1203–1212

44. Kaneto H, Matsuoka T-A. Down-regulation of pancreatic transcription factors and incretin receptors in type 2 diabetes. World J Diabetes 2013;4:263–269

45. Bjursell M, Admyre T, Göransson M, et al. Improved glucose control and reduced body fat mass in free fatty acid receptor 2-deficient mice fed a high-fat diet. Am J Physiol Endocrinol Metab 2011;300:E211–E220